Clim. Past Discuss., 10, 859–894, 2014
www.clim-past-discuss.net/10/859/2014/
doi:10.5194/cpd-10-859-2014

Climate of the Past
Discussions
Open Access

Tree-ring reconstruction of seasonal mean minimum temperature at Mt. Yaoshan, China, since 1873 and its relevance to 20th-century warming

Y. Liu[1,2], Y. Zhang[1,3], H. Song[1,3], Y. Ma[1,3], Q. Cai[1], and Y. Wang[2,1,3]

[1]The State Key Laboratory of Loess and Quaternary Geology, Institute of Earth Environment, Chinese Academy of Sciences, Xi'an 710075, China
[2]School of Human Settlement and Civil Engineering, Xi'an Jiaotong University, Xi'an 710049, China
[3]The University of the Chinese Academy of Science, Beijing 100049, China

Received: 26 December 2013 – Accepted: 25 February 2014 – Published: 6 March 2014

Correspondence to: Y. Liu (liuyu@loess.llqg.ac.cn)

Published by Copernicus Publications on behalf of the European Geosciences Union.

Abstract

It is very important to comprehend the climate variations in the vast regions of Central Plains of China. Current knowledge about climate changes of the past few hundred years in this region is primarily based on historical documents, and lack of evidences from the natural archives. However, these documents had somewhat artificially effects caused by the recorders, and not sufficient to fully understand natural climatic changes. In this paper, based on a significant correlation between the tree-ring width of Chinese Pine and observed instrumental data in the Mt. Yaoshan, China, we formulated a transfer function to reconstruct the mean minimum temperature (MMinT) from the previous December to the current June ($T_{\text{min\_DJ}}$) for the period 1873–2011. The reconstruction explained 39.8 % of the instrumental variance during the calibration period of 1958–2011. High $T_{\text{min\_DJ}}$ intervals with values greater than the 139 year average occurred in 1932–1965 and 1976–2006. The intervals 1878–1894 and 1906–1931 experienced a $T_{\text{min\_DJ}}$ lower than the 139 year average. The ten highest $T_{\text{min\_DJ}}$ years occurred after the 1950s, especially after 1996. A distinct upward trend in the $T_{\text{min\_DJ}}$ series beginning in the 1910s was apparent, and the highest value occurred around 2000. The 20th-century warming signal was captured well by the Yaoshan $T_{\text{min\_DJ}}$ temperature reconstruction, indicating that the temperature rise in the sensitive Central Plains of China region reflected the global temperature change. The $T_{\text{min\_DJ}}$ reconstruction also matched several other temperature series in China with similar warm-cold patterns. The distinct spatial correlation between both observed and reconstructed series and CRU TS3.10 grid data indicates that our results may represent $T_{\text{min\_DJ}}$ changes on a larger scale. The spatial correlation with sea surface temperature (SST) indicated that observed and reconstructed $T_{\text{min\_DJ}}$ temperatures in the Mt. Yaoshan are closely linked to the West Pacific, Indian and North Atlantic Oceans as well as El Niño-Southern Oscillation (ENSO).

CPD
10, 859–894, 2014

1 Introduction

In addition to genetic factors, tree growth is affected by environmental variables, such as temperature, precipitation and light. As a result, annual climatic information can be obtained from tree rings. Tree-ring data have played a crucial role in paleoclimatic research and global climate studies because of their high resolution, precise dating, high continuity and ease of sampling. The knowledge of the Northern Hemisphere temperature changes over the past 2000 years was primarily obtained through tree-ring data (Briffa et al., 2001, 2008; Esper et al., 2002; Mann et al., 2008). By using tree rings, series of temperature (Gou et al., 2008; Liang et al., 2008; Liu et al., 2009a, b, 2013; Cai et al., 2010, 2013; Bao et al., 2012; Li et al., 2013; Zhang et al., 2013) have been elucidated in China. A significant warming occurred in the late 20th century was detected in many researches based on tree-ring in China (Gou et al., 2008; Liu et al., 2009a, 2011). However, most dendroclimatological research in China has focused on the Tibetan Plateau and the northern arid to semi-arid regions. In other regions, such as the Central Plains of China (CPC), just few tree-ring studies have been conducted (Shi et al., 2009; Tian et al., 2009). The lack of dendroclimatological research in the CPC is mainly attributed to the difficulty of finding old trees. Nevertheless, it is very important to comprehend the climate variations in the vast regions of Central Plains of China. Current knowledge about climate changes of the past few hundred years in this region is primarily based on historical documents (Ge et al., 2002; Su, 2003). However, these documents have many disadvantages, for example, somewhat artificially effects caused by the recorders resulting in that the documents could not reflect the real natural climatic changes (Liu et al., 2001, 2003, 2007). Thus, it is necessary to investigate the natural climate changes in the CPC using natural archives, such as tree rings.

In this study, we reconstructed the mean minimum temperature from the previous December to the current June (T_{min_DJ}) beginning in 1873 AD based on *Pinus tabulaeformis* tree-ring widths from the Mt. Yaoshan in the CPC. The reconstructed T_{min_DJ} series was also used to explore the temporal and spatial representativeness of these data on a larger scale. This would be the first time to reconstruct the seasonal mean minimum temperature using tree rings in the CPC, which is helpful to understand the mechanism of climate change and evaluate its social and economic effects in the vast CPC region. This research is also vital to establish the tree ring network in China.

2 Materials and methods

2.1 Sampling

The Mt. Yaoshan is located in western Lushan, Henan Province (China), with an elevation range from 1300 m to 2153 m a.s.l. The mountain is in a transition region between the northern subtropical climate and a warm temperate continental monsoon climate. Over 50 years of meteorological observations indicate that the average annual precipitation is 823 mm, and most of the rainfall occurs from June to August. The annual mean temperature is approximately 14.8 °C. The warmest month is July, with temperatures ranging from 25.3 °C to 28.1 °C. The coldest month is January, with a temperature of approximately −1.9 °C. The dominant tree species within the sampling site is Chinese Pine (*Pinus tabulaeformis* Carr.). According to previous research (Xu, 1993), the cambial cell division of *Pinus tabulaeformis* begins at a mean temperature of 9.3 °C and ends at 15.9 °C. This temperature range occurs from late April to mid-September in the Mt. Yaoshan. Broad-leaf tree species in the area include *Quercus aliena* var. *acuteserrata* and *Betula albo-sinensis.*

We selected *Pinus tabulaeformis* Carr. as our study species at a site located at 33°43′ N, 112°16′ E, with an elevation of 2010 m (Fig. 1). According to the standard of the International Tree-Ring Data Bank (ITRDB), two cores were recovered from each individual tree. A total of 61 cores from 31 living trees were sampled using 5 mm increment borers. This group of samples was named YS. All sampled trees had a discontinuous canopy. The soil at the sampling site was thick, brown mountain soil with a 30–40 cm depth.

CPD
10, 859–894, 2014

2.2 Chronology development

In the laboratory, all tree-ring samples were dried, fixed, surfaced and mounted according to the standard dendrochronological procedures. After cross-dating and measuring ring widths with 0.01 mm precision, the tree ring of each sample was assigned an exact calendar year. The COFECHA program (Holmes, 1983) was used to control the quality of the cross-dating. To eliminate the effect of the tree age and obtain more low-frequency signals, we used the regional curve standardization (RCS) (Briffa et al., 1992) method to process the tree-ring width series during the chronology development. First, we aligned the individual tree-ring series by cambial age to represent the overall age-related growth trend in the Yaoshan region. The curve obtained by averaging these series year by year reflected age-related biological noise. Departures of the raw measurement from the regional curve (RC) were considered as a result of climatic forcing. The new RC growth anomalies were re-aligned by calendar year to produce the final RCS chronology. To utilize the maximum length of the tree-ring chronology and to assure the reliability of the reconstruction, the chronology was restricted to the period 1873–2011 with a sub-sample signal strength (SSS) (Wigley et al., 1984) of at least 0.80 (Fig. 2). The statistical characteristics of the YS RCS chronology are shown in Table 1.

2.3 Meteorological and PDSI data

In this study, we used the observed data from the Xixia (33°18′ N, 111°30′ E, 250.3 m, 1957–2011) and Lushi (34°03′ N, 111°02′ E, 568.8 m, 1952–2011) meteorological stations. The Baofeng (33°53′ N, 111°03′ E, 136.4 m, 1957–2011) and Nanyang (33°02′ N, 112°35′ E, 129.2 m, 1952–2011) stations were chosen as references. Standard methods were used to test the homogeneity and randomness of the observed meteorological data (Potter, 1981; Peterson and Easterling, 1994; Easterling and Peterson, 1995). The results indicated that the temperature and precipitation data from the Xixia and Lushi meteorological stations qualified for further analysis. The distributions of the

CPD
10, 859–894, 2014
Tree-ring reconstruction
Y. Liu et al.

monthly mean temperature, mean minimum temperature, mean maximum temperature and precipitation of each station are shown in Fig. 3. The climate factor variations match well among the four meteorological stations (e.g., the peaks of temperature and precipitation occur in July).

To better understand regional climate characteristics, the meteorological data from the Lushi and Xixia stations were averaged to represent regional climate conditions. As described in the following section, the YS chronology and the averaged meteorological data were used to perform a correlation analysis. We used the monthly mean temperature, mean minimum temperature, mean maximum temperature and precipitation as climatic variables in the correlation analysis.

To determine the combined effects of precipitation and temperature, we also analyzed the relationship between ring widths and PDSI. The PDSI is a standardized measure of surface moisture conditions (Palmer, 1965) and efficiently reflects drought variations. The PDSI data used in this study were obtained from the global PDSI dataset developed by Dai et al. (2004), which features a 2.5° × 2.5° grid system. We selected the data from the grid point at 33.75° N, 112.25° E (1957 to 2009), which was located nearest to our sampling site.

2.4 Statistical methods

We used a correlation function to explore the relationship between the tree-ring width index and observed meteorological data. This function was also used to explore the relationships between our reconstruction, alternative temperature proxies and large-scale temperature reconstructions.

To test the stability of the correlations, the leave-one-out test (Mosteller and Tukey, 1977) was used. This test involves calculating the correlation of the remaining time series after gradually removing the values for one year throughout the entire time period to examine the existence of outliers.

A traditional split calibration-verification method was used to test the stability and reliability of the regression equation (Fritts, 1991; Cook et al., 1999). The calibration was

Discussion Paper | Discussion Paper | Discussion Paper | Discussion Paper |

CPD

10, 859–894, 2014

Tree-ring reconstruction

Y. Liu et al.

independently conducted in both the 1957–1986 and 1982–2011 periods, and the verification was performed on the periods not included in the calibration (i.e., 1987–2011 and 1957–1981). The parameters used in this method were Pearson's correlation coefficient (r), the sign test (S), the reduction error (RE) and the coefficient of efficiency (CE). The RE tests whether a reconstruction provides a better estimate of climatic variability than simply using the mean climatology in the calibration period (Cook and Kairiukstis, 1990; Cook et al., 1994). The values of the RE range from negative infinity to 1.0 (a perfect estimation). The CE is used to determine the model skill during the verification period (not the calibration period). The CE can be described as an expression of the true r^2 of a regression model when applied to a new dataset (Cook and Kairiukstis, 1990; Cook et al., 1994). The CE values also range from negative infinity to 1.0 (a perfect estimation). The values of the RE and CE greater than zero indicate rigorous model skill. For the RE and CE values, higher positive values are more favorable. Typically, the CE values are lower than those of the RE. However, compared with the RE, the CE is a more rigorous verification statistic (Cook et al., 1999).

The effective number of degrees of freedom (EDOF) for each pair of smoothed time series was estimated following Fritts (1976).

To examine the regional representativeness of the temperature reconstruction, a spatial correlation analysis was performed using the KNMI climate explorer (http://climexp.knmi.nl). Other tree-ring width-based temperature reconstructions from the source region of Yangtze River, Zhen'an and Mt. Funiushan were compared with our minimum temperature reconstruction for the past 139 years. A spectral analysis was performed using a multi-taper method, which is especially powerful for short time series (Mann and Lees, 1996; Rigozo et al., 2002).

CPD
10, 859–894, 2014

3 Results

3.1 Correlations between YS ring width and climatic data

Canonical dendroclimatology assumes that the climate in year $t-1$ affects the ring width in the following year t (Fritts, 1976). Thus, the climatic variables were obtained from the previous September to the current September for this study.

We calculated the Pearson correlation between the ring width index and the meteorological data to assess the response of tree growth to climatic factors prior to and during the growing season. The results suggest that there were no significant correlations between tree-ring width and precipitation. The sampling site is located in a monsoon area and has a relatively high elevation; thus, precipitation is sufficient for tree growth. In terms of temperature, the ring width index was poorly correlated with the monthly mean temperature and mean maximum temperature. In contrast, the ring width indices were positively correlated with the mean minimum temperature from the previous September to the current September, except in the previous October (Fig. 4). By month, the highest correlation was found between the ring width index and the mean minimum temperature of the previous December to the current June ($T_{\text{min\_DJ}}$), with $r = 0.631$ ($p < 0.001$, $N = 54$). Clearly, a linear relationship existed between the $T_{\text{min\_DJ}}$ and the tree-ring width (Fig. 5).

The correlations between the monthly PDSI data and the ring width indices were not significant in every month. Therefore, we did not analyze the PDSI data in the following sections.

3.2 Transfer function and verification

Based on the correlation between the YS tree-ring width index and the observed $T_{\text{min\_DJ}}$, a simple linear regression model was created to reconstruct the climate from

Discussion Paper | Discussion Paper | Discussion Paper | Discussion Paper |

CPD
10, 859–894, 2014

Tree-ring reconstruction

Y. Liu et al.

the tree rings:

$$T_{\text{min\_DJ}} = 1.547W_t + 3.666 \quad (1)$$

$$(N = 54;\ r = 0.631;\ R^2 = 39.8\,\%;\ R^2_{\text{adj}} = 38.7\,\%;\ F = 34.40;\ p < 0.0001;\ \text{D/W} = 1.68)$$

where $T_{\text{min\_DJ}}$ is the mean minimum temperature from the previous December to the current June and W_t is the associated tree-ring width index of the YS RCS chronology in the year t. During the calibration period of 1958–2011, the predictor variable accounted for 38.7 % of the variance, adjusted for the loss of degrees of freedom in the $T_{\text{min\_DJ}}$ temperature data. The Durbin–Watson statistic (D/W), used to detect the presence of autocorrelation in the residuals from a regression analysis, was 1.68. This value indicates that autocorrelation did not occur among our residuals (when $N = 54$, autocorrelation did not occur with the D/W values of 1.57–2.43) (Durbin and Watson, 1950). A comparison between reconstructed and observed $T_{\text{min\_DJ}}$ during 1958–2011 is shown in Fig. 6, indicating that the reconstructed $T_{\text{min\_DJ}}$ tracked the observations very well.

The results of the split calibration-verification method (Table 2) indicated that the correlation coefficient and product means between the actual and reconstructed $T_{\text{min\_DJ}}$ in all calibration and verification periods were significant at the 0.01 level. The results of the sign test were statistically significant in all calibration and verification periods ($p < 0.05$). The RE and CE values in both verification periods were positive, indicating that the regression model had good predictive performance and was efficient in reconstructing $T_{\text{min\_DJ}}$ for the Yaoshan region.

However, the leave-one-out test results suggested that 2007 was an outlier from the model. If we omit this year, the explained variance of the $T_{\text{min\_DJ}}$ temperature rises to 48.1 %, and all tests of the split calibration-verification results are significantly improved (Table 3). The observed data indicated that there was an extremely cold event during 3–4 April 2007, with a minimum temperature of −3.1 °C (the mean minimum temperature in April of 2007 was 7.4 °C). Clearly, the extremely low temperatures during 3–4 April 2007 affected the tree growth. Although 2007 was an unusual year, we

CPD
10, 859–894, 2014

did not remove it from the model (1) because we cannot discount the possibility that similar events have happened in the past.

After applying a five year moving average to the reconstruction and observation (Fig. 7), the correlation coefficient increased, with $r = 0.835$, $p < 0.01$ and $R^2 = 69.7\,\%$. After reducing the degrees of freedom, the effective number of degrees of freedom was 9, and $r_{p=0.01}(9) = 0.735$. This finding demonstrates that the reconstruction is more reliable for providing estimates of natural variability on decadal time scales (D'Arrigo et al., 1998; Cook et al., 2000).

3.3 $T_{\text{min\_DJ}}$ reconstruction since 1873 in the Mt. Yaoshan

Overall, all test results sufficiently demonstrated the validity of our regression model (1). Therefore, we used the full instrumental period $T_{\text{min\_DJ}}$, spanning 54 years, to develop the final reconstruction. Based on the regression model (1), the $T_{\text{min\_DJ}}$ for 1873–2011 in the Mt. Yaoshan was reconstructed and is presented in Fig. 8. The smoothed line represents the ten year low-pass data, and the horizontal line represents the mean for 1873–2011, with a value of 5.2 °C and a standard deviation (σ) ± 0.4 °C.

3.4 Spatial correlation and periodicities

The spatial correlation between our $T_{\text{min\_DJ}}$ reconstruction and the CRU TS3.10 MMinT datasets for the period 1958–2009 is shown in Fig. 9. Figure 9a (top) illustrates the spatial correlation between the observed $T_{\text{min\_DJ}}$ averaged from the Xixia and Lushi stations and the CRU TS3.10 $T_{\text{min\_DJ}}$ datasets (1958–2009). Figure 9b (bottom) provides the correlation between the reconstructed $T_{\text{min\_DJ}}$ in the Yaoshan region with $T_{\text{min\_DJ}}$ of CRU TS3.10.

The periodicity test revealed remarkable $T_{\text{min\_DJ}}$ temperature reconstruction quasi-cycles of 78.7, 44.4, 35.3, 27, 6.6, 4.3, 3.5 and 3.0 years at the 95 % confidence level for the past 139 years (Fig. 10).

CPD
10, 859–894, 2014

CPD
10, 859–894, 2014

4 Discussions

The high correlation between tree ring width index and the mean minimum temperature of previous December to current June is logical and easy to understand. During the winter, increased minimum temperature protects roots and cambial cells from cold damage (Pederson et al., 2004). On the other hand, relatively higher minimum temperature in spring may result in increasing soil water and extending growing season, which would produce a wide ring. The influence of winter-spring temperatures on tree growth was also observed in *Pinus massoniana* and *Pinus taiwanensis* in southeastern China (Shi et al., 2013; Duan et al., 2012).

In the T_{min_DJ} reconstruction, the low-pass curve exhibited a gradual increasing trend, with a slope of 0.054 °C/decade from 1910 to 2011. This result was consistent with reports from the Intergovernmental Panel on Climate Change (IPCC, 2007), which found that 20th-century global warming began around 1910. The increasing trend was more obvious from 1965 to 2011, with a slope of 0.123 °C/decade. This increasing rate was quite similar to that of Nanwutai (300 km west of Yaoshan, at 0.117 °C/decade) (Liu et al., 2014). In this study, we defined a "high T_{min_DJ} year" as > 5.6 °C (mean + σ) and a "low T_{min_DJ} year" as < 4.8 °C (mean – σ). The values of high and low T_{min_DJ} in the reconstruction were 17 and 21, accounting for 12.2 % and 15.1 % of the entire series, respectively. The ten highest and ten lowest T_{min_DJ} values among the 139 years are listed in Table 3. Many of the highest T_{min_DJ} years appeared after the 1950s, especially after 1996.

We smoothed the original series by an 11 year moving average to obtain the low-frequency variation of the T_{min_DJ} reconstruction. After smoothing, two cold periods were apparent (1878–1894 and 1906–1931), with T_{min_DJ} values lower than the 139 year mean. Two distinct warm intervals, with T_{min_DJ} values higher than the 139 year mean, occurred during the periods 1932–1965 and 1976–2006. Warming during the 20th century was well represented in the T_{min_DJ} temperature reconstruction of the Mt. Yaoshan. These results indicate that the mean minimum temperature increase in the

Central Plains of China (CPC) was synchronized with the rise of the global temperature and that the CPC is sensitive to global climate change. Previous studies revealed that recent warming trends in China not only occurred in winter (Chen et al., 2012; Shi et al., 2013) but also in summer (i.e., May to July) (Liu et al., 2014). Thus, it is logical that the T_{min_DJ} in the CPC displayed a rising trend because it represents winter and summer. However, the T_{min_DJ} reconstruction in the Mt. Yaoshan also showed a decreasing trend in the 21st century.

The T_{min_DJ} reconstruction of the Mt. Yaoshan could be compared with several other temperature series from different regions of China, such as the March–April mean temperature in Zhen'an in the south-central Qinling Mountains (Liu et al., 2001), the previous December to current April mean temperature at Mt. Funiushan (Shi et al., 2009) and the June–August minimum temperature at the source region of the Yangtze River (Liang et al., 2008) (Fig. 11). All of these series displayed synchronized variations and similar warm-cold intervals, indicating that the temperature variations in the Mt. Yaoshan were consistent over a significantly large spatial scale. Although these comparison regions were far from the sampling site (Fig. 1), they showed highly synchronous warming trends in the late 20th century. Another notable feature was that all curves exhibited significantly low temperatures around 1880.

Although the months varied in the previous comparisons, the conclusions are supported by the significant correlation between the T_{min_DJ} in the Yaoshan region and other times of the year. Correlation analysis indicated that the T_{min_DJ} was significantly correlated with the mean temperature from March to April ($N = 54$, $r = 0.60$, $p < 0.01$), with the mean temperature from the previous December to the current April ($N = 53$, $r = 0.81$, $p < 0.001$) and with the mean minimum temperature from June to August ($N = 54$, $r = 0.29$, $p < 0.05$). These calculations indicated that the T_{min_DJ} was consistent with other temperature variables in different seasons. Thus, the T_{min_DJ} reconstruction in this study could be compared with the temperature series used in Fig. 11.

The close spatial relationship that our T_{min_DJ} reconstruction displayed could be demonstrated by using CRU TS3.10 MMinT datasets to calculate the correlation for

CPD
10, 859–894, 2014

the period 1958–2009 (Fig. 9). The reconstructed and instrumental data exhibited similar patterns, indicating that our temperature reconstruction represented reliable climate variations on a large scale. The reconstruction had a significant positive correlation with most of China (especially eastern China), the Korean peninsula, western Japan and the Mongolian Plateau (Fig. 9).

The spatial calculation also indicated that the Mt. Yaoshan's observed and reconstructed $T_{\text{min\_DJ}}$ were significantly correlated with the mean December–June SSTs of the western Pacific, Indian and North Atlantic Oceans (Fig. 12). The SSTs in the ENSO region were also correlated with the Yaoshan $T_{\text{min\_DJ}}$ temperature (Fig. 12).

We compared the $T_{\text{min\_DJ}}$ temperature reconstruction with El Niño events recorded since 1880 (Gergis and Fowler, 2009). The comparison revealed that 19 of the 26 major events corresponded to a $T_{\text{min\_DJ}}$ higher than the 11 year moving average, and the remaining seven events corresponded to lower $T_{\text{min\_DJ}}$ values. Of the seven extremely strong El Niño events, only one dropped below the average. The other events were above average since 1960 (Fig. 13). In general, the $T_{\text{min\_DJ}}$ over the Mt. Yaoshan region (or the CPC) was high during El Niño events.

Among the periodicities, the 78.7 year cycle corresponds to an oscillation in the global climate system of 60–80 years (i.e., an internal oscillation in the atmosphere–ocean system) (Schlesinger and Ramankutty, 1994; Qian and Lin, 2009). The 44.4 year cycle may be related to an oscillation in the climate system of 40–50 years that accounts for the irregular oscillations of the thermohaline circulation in the North Atlantic (Greatbatch and Zhang, 1995; Qian and Lin, 2009). The 35.3 year cycle corresponded to the Bruckner cycle, which accounts for solar activity (Raspopov et al., 2004). The 27 year cycle likely corresponded to sunspot activity (Han and Han, 2002). Additionally, the correlation between the reconstructed $T_{\text{min\_DJ}}$ and sunspot number series, after 11 year smoothing, reached 0.557 (EDOF = 11, $r_{p=0.05}(11) = 0.553$). Finally, the 3.0- to 6.6 year cycles resembled the ENSO cycle (Torrence and Webster, 1999), indicating that the $T_{\text{min\_DJ}}$ variation in the Mt. Yaoshan region was affected by ENSO. This was also observed in Fig. 12.

5 Conclusions

Using the tree-ring width of *Pinus tabulaeformis,* the mean minimum temperature of the previous December to the current June has been reconstructed in the Mt. Yaoshan, Central Plains of China for the past 139 years. The reconstruction explained 39.8 % of the instrumental variance during the calibration period (38.7 %, when adjusted for the loss of degrees of freedom). Warming during the 20th century was well-represented in the Yaoshan $T_{\text{min\_DJ}}$ reconstruction. Since the 1910s, the $T_{\text{min\_DJ}}$ presented a distinct increasing trend. The temperature peaked in 2000, which is consistent with the IPCC report that modern global warming began in the 1910s. Therefore, the temperature rise in the Central Plains of China was synchronized with the global temperature change. It is also apparent that the Central Plains of China are sensitive to global temperature change. Over the entire time series, the ten highest $T_{\text{min\_DJ}}$ years occurred after the 1950s, especially after 1996. The spatial correlations showed that the $T_{\text{min\_DJ}}$ values in the Mt. Yaoshan were able to reflect climate change on a larger spatial scale. The $T_{\text{min\_DJ}}$ in the Mt. Yaoshan was mainly influenced by solar activity; the mean December–June SSTs of the western Pacific, Indian and North Atlantic Oceans; and ENSO activity.

Acknowledgements. We thank Baofa Shen for his valuable help. This study was supported by grants from the CAS/SAFEA International Partnership Program for Creative Research Teams (KZZD–EW–TZ–03), the Chinese Academy of Sciences (KZZD–EW–04–01), the National Basic Research Program of China (no. 2013CB955900), the CAS Hundred Talents Program, the Key Project of the Institute of Earth Environment and the Project of State Key Laboratory of Loess and Quaternary Geology (SKLLQG), National Natural Science Foundation of China (41171170). This research is an initiative of the Sino-Swedish Tree-Ring Research Center (SISTRR): Contribution (No. 024).

References

Bao, G., Liu, Y., and Linderholm, H. W.: April–September mean maximum temperature inferred from Hailar pine (Pinus sylvestris var. mongolica) tree rings in the Hulunbuir region, Inner Mongolia, back to 1868 AD, Palaeogeogr. Palaeocl., 313, 162–172, 2012.

Briffa, K. R., Jones, P. D., Bartholin, T. S., Eckstein, D., Schweingruber, F. H., Karlen, W., Zetterberg, P., and Eronen, M.: Fennoscandian summers from AD 500: temperature changes on short and long timescales, Clim. Dynam., 7, 111–119, 1992.

Briffa, K. R., Osborn, T. J., Schweingruber, F. H., Harris, I. C., Jones, P. D., Shiyatov, S. G., and Vaganov, E. A.: Low-frequency temperature variations from a northern tree ring density network, J. Geophys. Res.-Atmos., 106, 2929–2941, doi:10.1029/2000jd900617, 2001.

Briffa, K. R., Shishov, V. V., Melvin, T. M., Vaganov, E. A., Grudd, H., Hantemirov, R. M., Eronen, M., and Naurzbaev, M. M.: Trends in recent temperature and radial tree growth spanning 2000 years across northwest Eurasia, Philos. T. Roy. Soc. B, 363, 2271–2284, doi:10.1098/rstb.2007.2199, 2008.

Cai, Q. F., Liu, Y., Bao, G., Lei, Y., and Sun, B.: Tree-ring-based May–July mean temperature history for Luliang Mountains, China, since 1836, Chinese Sci. Bull., 55, 3008–3014, 2010.

Cai, Q. F., Liu, Y., and Tian, H.: A dendroclimatic reconstruction of May–June mean temperature variation in the Heng Mounatins, north China, since 1767 AD, Quatern. Int., 283, 3–10, 2013.

Chen, F., Yuan, Y. J., Wei, W. S., Yu, S. L., and Zhang, T. W.: Tree ring-based winter temperature reconstruction for Changting, Fujian, subtropical region of Southeast China, since 1850: linkages to the Pacific Ocean, Theor. Appl. Climatol., 109, 141–151, 2012.

Cook, E. R. and Kairiukstis, L. A.: Methods of Dendrochronology, Kluwer Academic Publishers, Dordrecht, 391 pp., 1990.

Cook, E. R., Briffa, K. R., and Jones, P. D.: Spatial regression methods in dendroclimatology – a review and comparison of two techniques, Int. J. Climatol., 14, 379–402, 1994.

Cook, E. R., Meko, D. M., Stahle, D. W., and Cleaveland, M. K.: Drought reconstructions for the continental United States, J. Climate, 12, 1145–1162, 1999.

Cook, E. R., Buckley, B. M., D'Arrigo, R. D., and Peterson, M. J.: Warm-season temperatures since 1600 BC reconstructed from Tasmanian tree rings and their relationship to large-scale sea surface temperature anomalies, Clim. Dynam., 16, 79–91, doi:10.1007/s003820050006, 2000.

Dai, A., Trenberth, K. E., and Qian, T. T.: A global dataset of Palmer Drought Severity Index for 1870–2002: relationship with soil moisture and effects of surface warming, J. Hydrometeorol., 5, 1117–1130, doi:10.1175/Jhm-386.1, 2004.
D'Arrigo, R. D., Cook, E. R., Salinger, M. J., Palmer, J., Krusic, P. J., Buckley, B. M., and Villalba, R.: Tree-ring records from New Zealand: long-term context for recent warming trend, Clim. Dynam., 14, 191–199, 1998.
Duan, J., Zhang, Q. B., Lv, L., and Zhang, C.: Regional-scale winter-spring temperature variability and chilling damage dynamics over the past two centuries in southestern China, Clim. Dynam., 39, 919–928, 2012.
Durbin, J. and Watson, G. S.: Testing for serial correlation in least squares regression, I, Biometrika, 37, 409–428, 1950.
Easterling, D. R. and Peterson, T. C.: A new method for detecting and adjusting for undocumented discontinuities in climatological time series, Int. J. Climatol., 15, 369–377, 1995.
Esper, J., Cook, E. R., and Schweingruber, F. H.: Low-frequency signals in long tree-ring chronologies for reconstructing past temperature variability, Science, 295, 2250–2253, doi:10.1126/science.1066208, 2002.
Fritts, H. C.: Tree Rings and Climate: Calibration, Academic Press, New York, 323–325, 1976.
Fritts, H. C.: Reconstructing Large-Scale Climatic Patterns from Tree-Ring Data, The University of Arizona Press, Tucson, 286 pp., 1991.
Ge, Q. S., Zheng, J. Y., Man, Z. M., Fang, X. Q., and Zhang, P. Y.: Reconstruction and analysis on the series of winter-half year temperature changes over the past 2000 years in eastern China, Earth Science Frontiers, 9, 169–181, 2002.
Gergis, J. L. and Fowler, A. M.: A history of ENSO events since AD 1525: implications for future climate change, Climatic Change, 92, 343–387, 2009.
Gou, X., Peng, J., Chen, F., Yang, M., Levia, D. F., and Li, J.: A dendrochronological analysis of maximum summer half year temperature variations over the past 700 years on the northeastern Tibetan Plateau, Theor. Appl. Climatol., 93, 195–206, 2008.
Greatbatch, R. J. and Zhang, S.: An interdecadal oscillation in an idealized ocean-basin forced by constant heat-flux, J. Climate, 8, 81–91, 1995.
Han, Y. B. and Han, Y. G.: Wavelet analysis of sunspot relative numbers, Chinese Sci. Bull., 47, 609–612, 2002.
Holmes, R. L.: Computer-assisted quality control in tree-ring dating and measurement, Tree-Ring Bulletin, 43, 69–78, 1983.

IPCC: Climate Change 2007: The Physical Science Basis, Cambridge University Press, Cambridge, UK and New York, USA, 2007.

Li, Q., Liu, Y., Song, H. M., Cai, Q. F., and Yang, Y. K.: Long-term variation of temperature over North China and its links with large-scale atmospheric circulation, Quatern. Int., 283, 11–20, 2013.

Liang, E. Y., Shao, X. M., and Qin, N. S.: Tree-ring based summer temperature reconstruction for the source region of the Yangtze River on the Tibetan Plateau, Global Planet. Change, 61, 313–320, doi:10.1016/j.gloplacha.2007.10.008, 2008.

Liu, Y., Ma, L. M., and Cai, Q. F.: March to April Mean tempeture reconstruction from tree rings for Zhen'an region, Advances in Nature Science, 11, 157–162, 2001.

Liu, Y., Cai, Q. F., Park, W. K., An, Z. S., and Ma, L. M.: Tree-ring precipitation records from Baiyinaobao, Inner Mongolia since A. D. 1838, Chinese Sci. Bull., 48, 1140–1145, 2003.

Liu, Y., Sun, J. Y., Yang, Y. K., Cai, Q. F., Song, H. M., Shi, J. F., An, Z. S., and Li, X. X.: Tree-ring-drived precipitation records from Inner Mongolia, China, since A. D. 1627, Tree-Ring Res., 63, 3–14, 2007.

Liu, Y., An, Z. S., Linderholm, H. W., Chen, D. L., Song, H. M., Cai, Q. F., Sun, J. Y., and Tian, H.: Annual temperatures during the last 2485 years in the mid-eastern Tibetan Plateau inferred from tree rings, Sci. China Ser. D, 52, 348–359, 2009a.

Liu, Y., Linderholm, H. W., Song, H., Cai, Q., Tian, Q., Sun, J., Chen, D., Simelton, E., Seftigen, K., Tian, H., Wang, R., Bao, G., and An, Z.: Temperature variations recorded in Pinus tabulaeformis tree rings from the southern and northern slopes of the central Qinling Mountains, central China, Boreas, 38, 285–291, doi:10.1111/j.1502-3885.2008.00065.x, 2009b.

Liu, Y., Cai, Q. F., Song, H. M., An, Z. S., and Linderholm, H. W.: Amplitudes, rates, periodicities and causes of temperature variations in the past 2485 years and future trends over the central-eastern Tibetan Plateau, Chinese Sci. Bull., 56, 2986–2994, doi:10.1007/s11434-011-4713-7, 2011.

Liu, Y., Wang, Y., Li, Q., Sun, J., Song, H., Cai, Q., Zhang, Y., Yuan, Z., and Wang, Z.: Reconstructed May–July mean maximum temperature since 1745 AD based on tree-ring width of Pinus tabulaeformis in Qianshan Mountain, China, Palaeogeogr. Palaeocl., 388, 145–152, 2013.

Liu, Y., Wang, Y., Li, Q., Song, H., Leavitt, S. W., Wang, R., Linderhlom, H. W., and An, Z.: Tree-ring stable carbon isotope-based May–July temperature reconstruction over Nanwutai,

China, for the past century and its record of 20th century warming, Quaternary Sci. Rev., revision submitted, 2014.
Mann, M. E. and Lees, J. M.: Robust estimation of background noise and signal detection in climatic time series, Climatic Change, 33, 409–445, 1996.
Mann, M. E., Zhang, Z. H., Hughes, M. K., Bradley, R. S., Miller, S. K., Rutherford, S., and Ni, F. B.: Proxy-based reconstructions of hemispheric and global surface temperature variations over the past two millennia, P. Natl. Acad. Sci. USA, 105, 13252–13257, 2008.
Mosteller, F. and Tukey, J. W.: Data Analysis and Regression: a Second Course in Statistics, Addison-Wesley Series in Behavioral Science, Addison Wesley Publishing Company, Reading, 1977.
Palmer, W. C.: Meteorological Drought, in: Weather Bureau Research Paper 45, US Department of Commerce, Washington DC, 45 pp., 1965.
Pederson, N., Cook, E. R., Jacoby, G., Peteet, D. M., and Griffin, K. L.: The influence of winter temperature on the annual radial growth of six northern range margin tree species, Dendrochronologia, 22, 7–29, 2004.
Peterson, T. C. and Easterling, D. R.: Creation of homogeneous composite climatological reference series, Int. J. Climatol., 14, 671–679, 1994.
Potter, K. W.: Illustration of a new task for detecting a shift in mean precipitation series, Mon. Weather Rev., 109, 2040–2045, 1981.
Qian, W. H. and Lin, X.: An integrated analysis of dry-wet variability in western China for the last 4–5 centuries, Adv. Atmos. Sci., 26, 951–961, 2009.
Raspopov, O. M., Dergachev, V. A., and Kolstrom, T.: Periodicity of climate conditions and solar variability derived from dendrochronological and other palaeoclimatic data in high latitudes, Palaeogeogr. Palaeocl., 209, 127–139, doi:10.1016/j.palaeo.2004.02.022, 2004.
Rigozo, N. R., Nordemann, D. J. R., Echer, E., Zanandrea, A., and Gonzalez, W. D.: Solar variability effects studied by tree-ring data wavelet analysis, Adv. Space Res., 29, 1985–1988, doi:10.1016/S0273-1177(02)00245-4, 2002.
Schlesinger, M. E. and Ramankutty, N.: Low-frequency oscillation – Reply, Nature, 372, 508–509, 1994.
Shi, J. F., Lu, H. Y., Wan, J. D., Li, S. F., and Nie, H. S.: Winter-half year temperature reconstruction of the last century using Pinus armandii franch tree-ring width chronology in the eastern Qinling Mountains, Quaternary Sci., 29, 831–836, 2009 (in Chinese).

CPD
10, 859–894, 2014
Tree-ring reconstruction
Y. Liu et al.

Shi, J. F., Cook, E. R., Li, J. B., and Lu, H. Y.: Unprecedented January–July warming recorded in a 178 year tree-ring width chronology in the Dabie Mountains, southeastern China, Palaeogeogr. Palaeocl., 381, 92–97, 2013.
Su, Q. Y.: Some issues about disasters in Henan in modern times, Yindu Journal, 55–59, 2003 (in Chinese).
Tian, Q. H., Liu, Y., Cai, Q. F., Bao, G., Wang, W. P., Xue, W. L., Zhu, W. J., Song, H. M., and Lei, Y.: The maximum temperature of May–July inferred from tree-ring in Funiu Mountain since 1874 AD, Acta Geogr. Sin., 64, 879–887, 2009 (in Chinese).
Torrence, C. and Webster, P. J.: Interdecadal changes in the ENSO-monsoon system, J. Climate, 12, 2679–2690, 1999.
Wigley, T. M. L., Briffa, K. R., and Jones, P. D.: On the average value of correlated time series, with application in dendroclimatology and hydrometeorology, J. Clim. Appl. Meteorol., 23, 201–213, 1984.
Xu, H. C.: Tree growth, in: Chinese pine, 125–126, China Forest Industry Press, Beijing, 1993 (in Chinese).
Zhang, T. W., Yuan, Y. J., Wei, W. S., Yu, S. L., Zhang, R. B., Shang, H. M., Chen, F., Fan, Z., and Qin, L.: Tree-ring-based temperature reconstruction for the northern Greater Higgnan Mountains, China, since AD 1717, Int. J. Climatol., 33, 422–429, doi:10.1002/Joc.3433, 2013.

CPD
10, 859–894, 2014

Table 1. Statistical characteristics of the YS RCS chronology.

Statistical item	RCS
Mean sensitivity	0.216
Standard deviation	0.329
Skewness	−0.134
Kurtosis	2.535
First order autocorrelation	0.658
Mean correlation between all series	0.386
Mean correlation between trees	0.379
Mean correlation within a tree	0.739
Signal noise ratio	30.225
Expressed population signal (EPS)	0.968
%Variance in 1st PC	30.15 %
First year where SSS > 0.80 (No. of Cores)	1873(13)

CPD
10, 859–894, 2014

Table 2. Statistics for a split calibration – verification procedure (including the year 2007).

Calibration Period	r	R^2	ST	t	Verification Period	r	R^2	RE	CE	ST	t
1958–1987	0.62	0.38	21[a]	5.12	1988–2011	0.51	0.26	0.47	0.07	19[b]	3.69
1982–2011	0.47	0.23	21[a]	4.63	1958–1981	0.72	0.52	0.60	0.47	18[a]	4.99
1958–2011	0.63	0.40	38[b]	7.37							

[a] significant at the 0.05 level (2-tailed).
[b] significant at the 0.01 level (2-tailed).

CPD
10, 859–894, 2014

Table 3. Statistics for a split calibration – verification procedure (excluding the year 2007).

Calibration Period	r	R^2	ST	t	Verification Period	r	R^2	RE	CE	ST	t
1958–1987	0.62	0.38	21[a]	5.12	1988–2011	0.68	0.46	0.62	0.34	19[b]	5.19
1981–2011	0.62	0.38	23[b]	5.93	1958–1980	0.72	0.51	0.60	0.51	18[a]	4.94
1958–2011	0.69	0.48	37[b]	7.40							

[a] significant at the 0.05 level (2-tailed).
[b] significant at the 0.01 level (2-tailed).

CPD
10, 859–894, 2014

Tree-ring reconstruction

Y. Liu et al.

Table 4. Ten highest and ten lowest T_{min_DJ} years in the 139 years reconstruction

Rank	Year	Warm (°C)	Year	Cold (°C)
1	2002	5.77	1881	3.95
2	2001	5.78	1880	4.01
3	1966	5.83	1882	4.09
4	1960	5.84	1883	4.25
5	1998	5.86	1879	4.28
6	2004	5.86	1918	4.39
7	1999	5.89	1884	4.43
8	1959	5.93	1877	4.44
9	2003	6.04	1878	4.45
10	2006	6.10	1885	4.45

CPD
10, 859–894, 2014

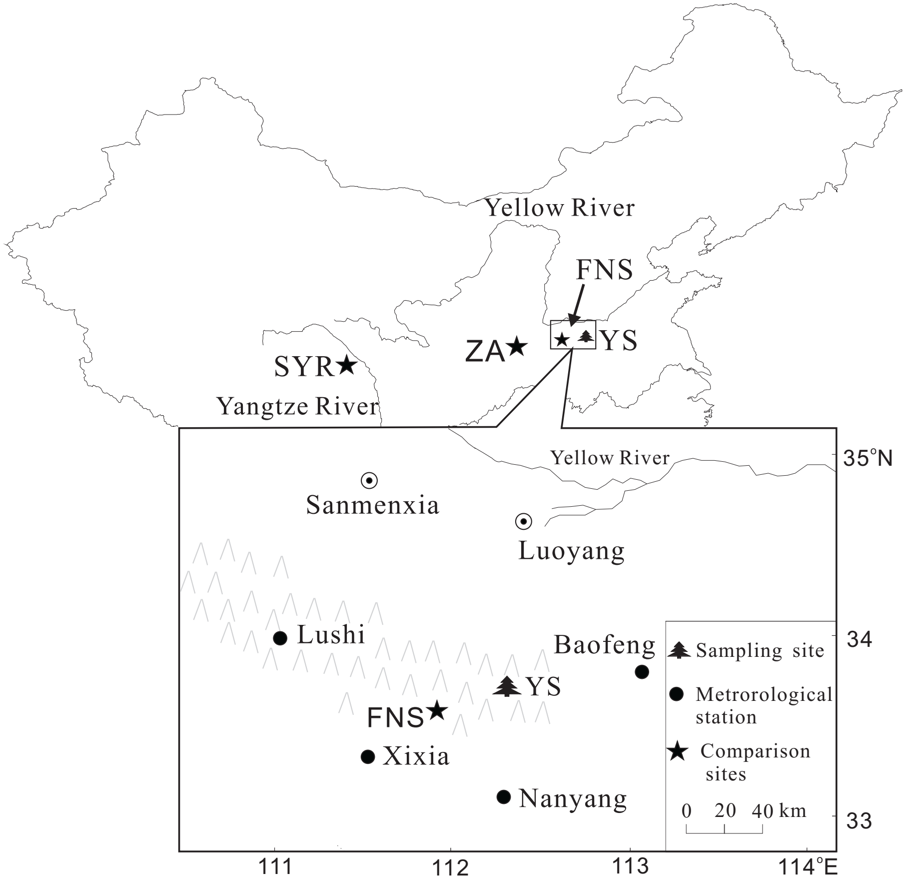

Fig. 1. Map of the sampling site (YS) and nearby meteorological stations. The dark stars are the tree-ring sites used for comparison with our reconstruction in this paper. SYR–Source region of the Yangtze River; ZA–Zhen'an; FNS–Mt. Funiushan.

CPD
10, 859–894, 2014

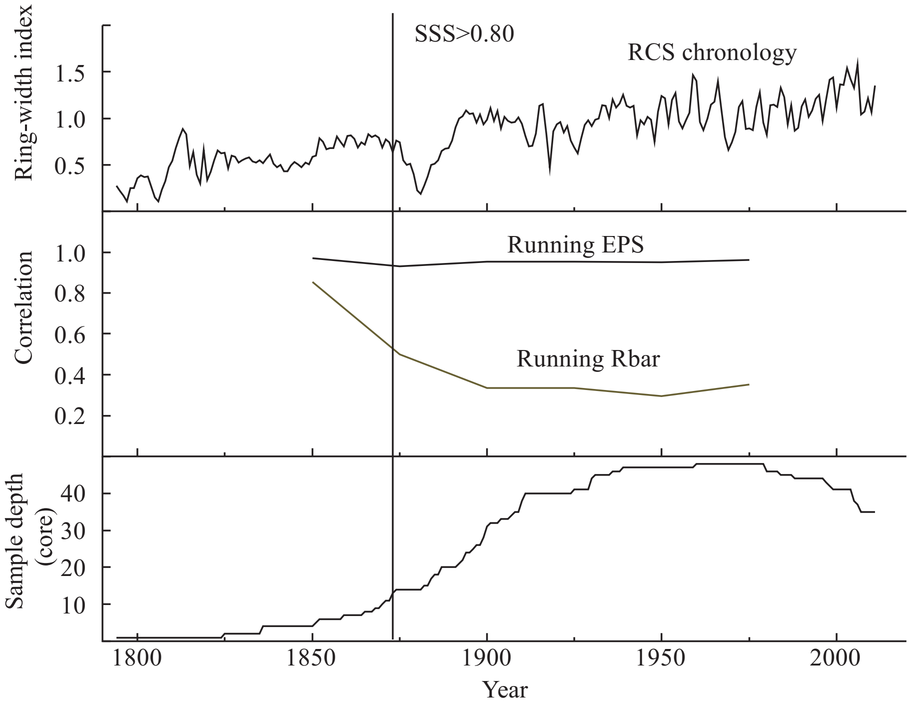

Fig. 2. A plot of the YS RCS chronology showing the expressed population signal (EPS), Rbar statistics and sample depth. (The Rbar–average correlation between the indices for each year over sequential time periods.)

CPD
10, 859–894, 2014

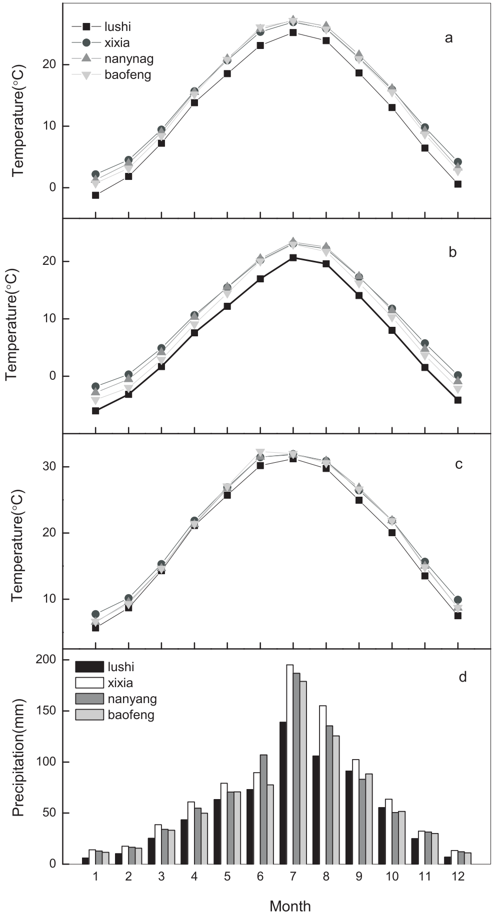

Fig. 3. Monthly mean temperature **(a)**, mean minimum temperature **(b)**, mean maximum temperature **(c)** and precipitation **(d)** from Xixia (1957–2011), Lushi (1952–2011), Baofeng (1957–2011) and Nanyang (1952–2011) meteorological stations.

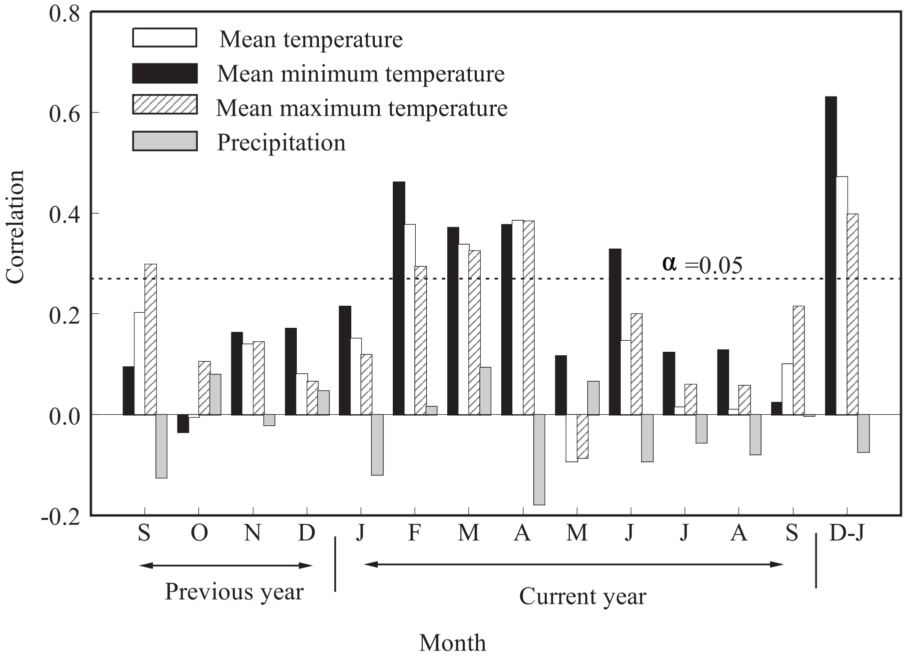

Fig. 4. Correlation between the ring width index and monthly averaged meteorological data from Lushi and Xixia stations during 1957–2011, including the mean temperature, mean maximum temperature, mean minimum temperature and precipitation. D–J: December–June.

CPD
10, 859–894, 2014

Tree-ring reconstruction

Y. Liu et al.

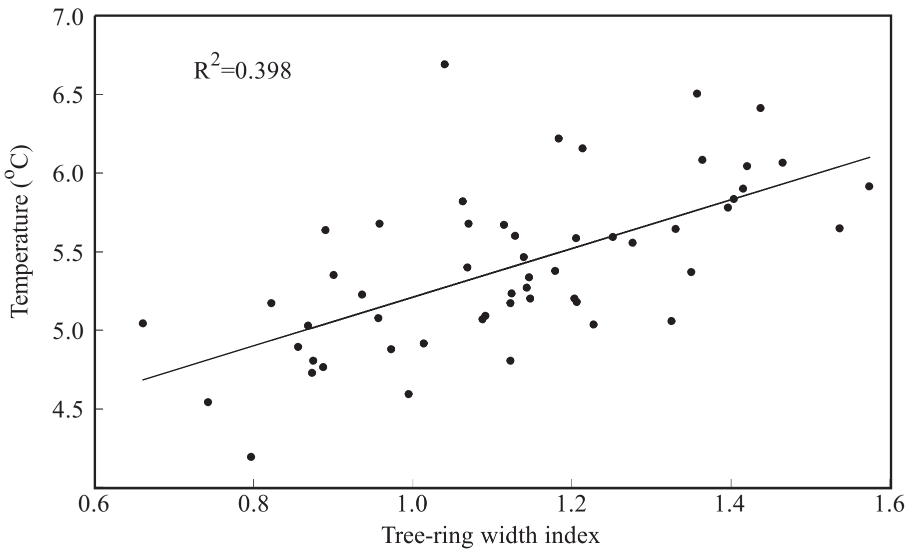

Fig. 5. Scatterplot of the tree-ring width index and the averaged December–June MMinT (1957–2011).

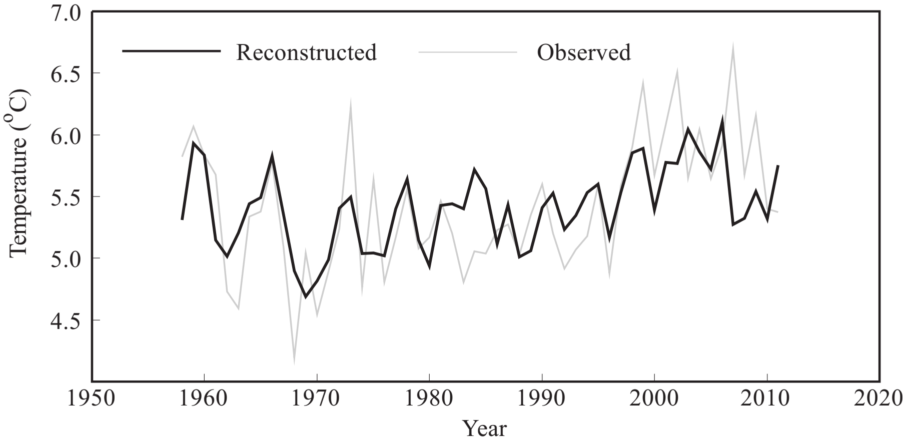

Fig. 6. Comparison between the observed (gray line) and reconstructed (black line) December–June MMinT (1958–2011).

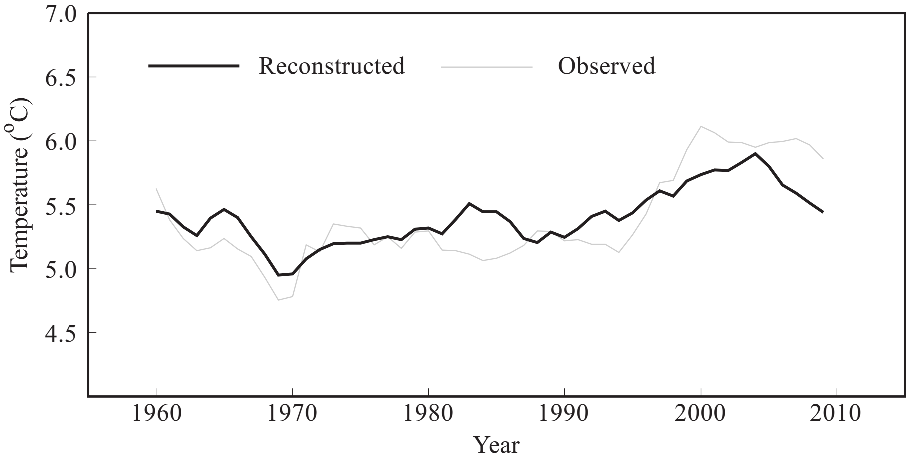

Fig. 7. Comparison between the actual instrumental data and the reconstructed T_{min_DJ} with a five year moving average (EDOF = 9, $r = 0.835$, $p < 0.01$, $R^2 = 0.697$, $r_{p=0.01}(9) = 0.735$).

CPD
10, 859–894, 2014

Title Page
Abstract | Introduction
Conclusions | References
Tables | Figures
◀| |▶
◀ ▶
Back | Close
Full Screen / Esc
Printer-friendly Version
Interactive Discussion

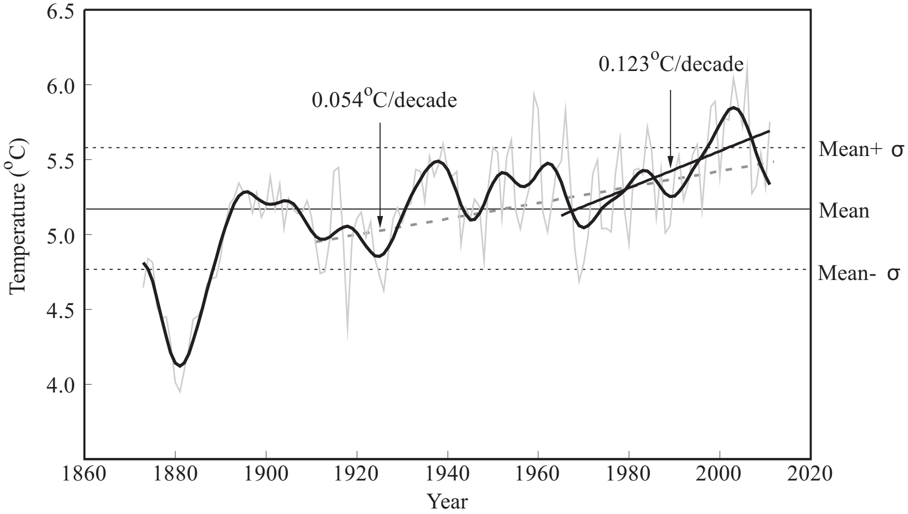

Fig. 8. Reconstructed mean minimum temperature from the previous December to the current June during 1873–2011 in the Mt. Yaoshan region. The mean was 5.2 °C from 1873 to 2011, and the standard deviation (σ) was ±0.4 °C. The bold line denotes the ten year low-passed data.

CPD
10, 859–894, 2014

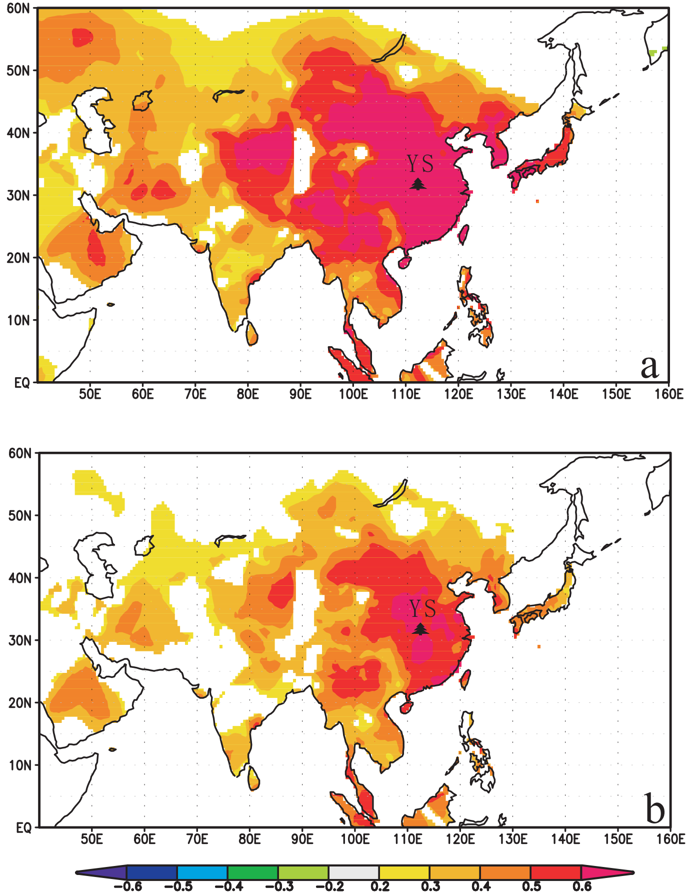

Fig. 9. Spatial correlations of the $T_{\text{min\_DJ}}$: **(a)** observed $T_{\text{min\_DJ}}$ with the $T_{\text{min\_DJ}}$ of CRU TS3.10; **(b)** reconstructed $T_{\text{min\_DJ}}$ in the Yaoshan region with the $T_{\text{min\_DJ}}$ of CRU TS3.10.

CPD
10, 859–894, 2014

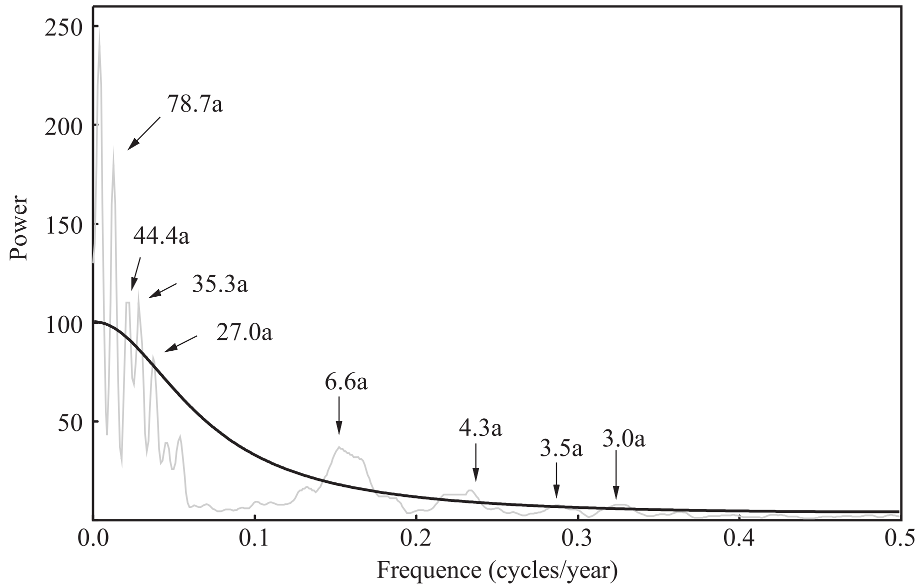

Fig. 10. Spectral density of the T_{min_DJ} reconstruction during 1873–2011 in the Yaoshan region. The dashed line is the 95 % confidence level.

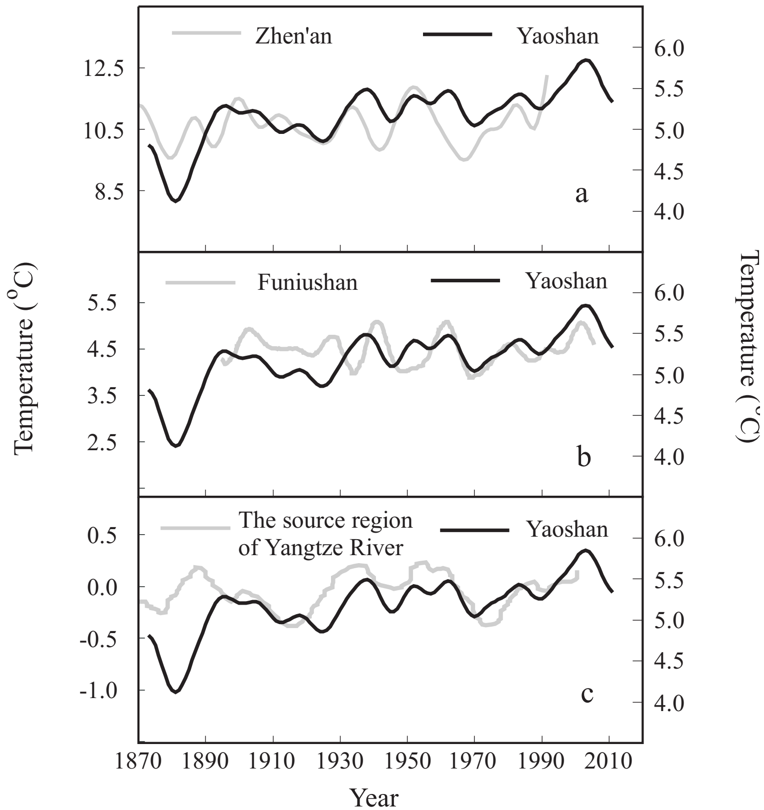

Fig. 11. Comparisons of the T_{min_DJ} reconstruction in the Mt. Yaoshan with alternate temperature series reconstructed with tree-ring widths. **(a)** March–April mean temperature in Zhen'an, South-Central Qinling Mountains (Liu et al., 2001). **(b)** Previous December to current April mean temperature at Mt. Funiushan (Shi et al., 2009). **(c)** June–August minimum temperature in the source region of the Yangtze River (Liang et al., 2008). All bold lines denote the ten year low-pass data.

CPD
10, 859–894, 2014

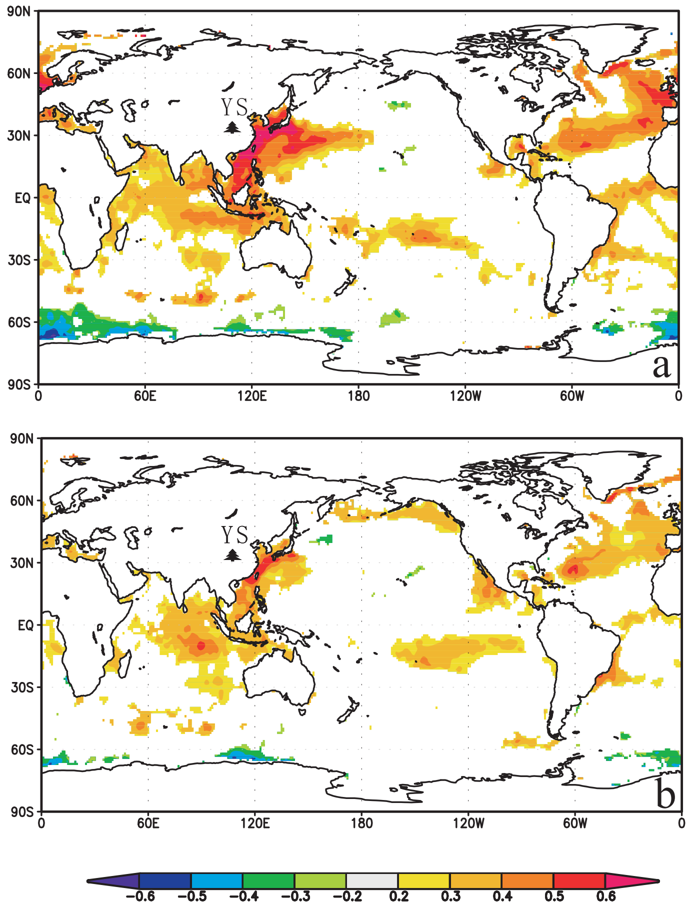

Fig. 12. The spatial correlations between the T_{min_DJ} and the December–June SSTs from 1958–2011. **(a)** Observed T_{min_DJ} and **(b)** reconstructed T_{min_DJ}.

CPD
10, 859–894, 2014

Title Page
Abstract | Introduction
Conclusions | References
Tables | Figures
◀| |▶
◀ ▶
Back | Close
Full Screen / Esc
Printer-friendly Version
Interactive Discussion

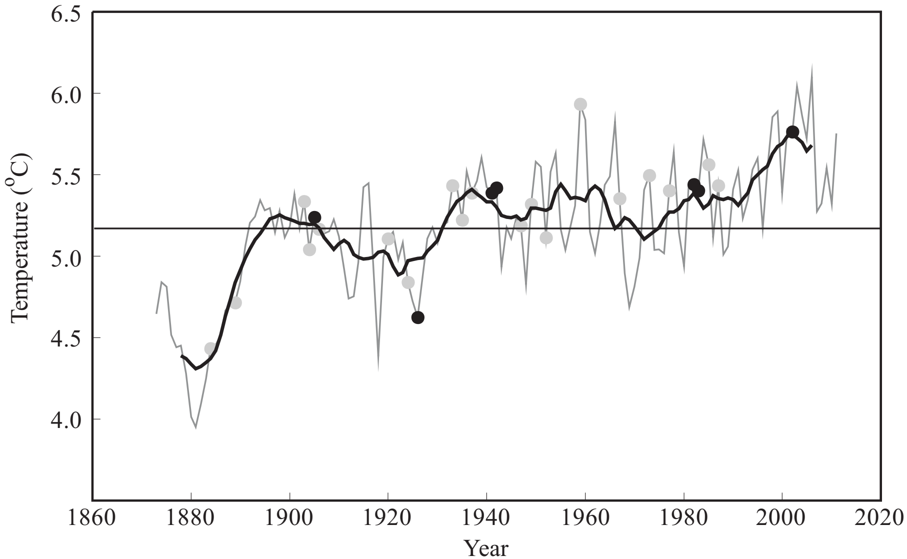

Fig. 13. Correspondence between El Niño events and the Yaoshan T_{min_DJ} reconstruction. The bold line is an 11 year moving average. Black dots represent extremely strong El Niño events, and grey dots represent strong El Niño events.

CPD
10, 859–894, 2014

Tree-ring reconstruction

Y. Liu et al.